PLASMA ELECTROLYTIC OXIDATION OF PURE TITANIUM

AT CONSTANT APPLIED VOLTAGE

By

HUNTER PITTS

Presented to the Faculty of the Graduate School of

The University of Texas at Arlington in Partial Fulfillment

of the Requirements

for the Degree of

MASTER OF SCIENCE IN MATERIALS SCIENCE AND ENGINEERING

THE UNIVERSITY OF TEXAS AT ARLINGTON

December 2021

ACKNOWLEDGEMENTS

I thank Dr. Meletis my Supervising Professor for his leadership and support during my research and studies. His knowledge and guidance were invaluable to my project and helped me to further my understanding of the research and in my classes as well. I also want to thank my committee members, Dr. Cao, and Dr. Jiang. Dr. Cao for his advice and assistance with the modeling portion of the project and Dr. Jiang for his advice and assistance in the characterization portion of the project.

Next, I would like to thank my fellow lab mates for their help in bouncing ideas off one another. I would like to thank Wisanu and Chuzhong for their help in training and teaching me how to use different devices in the lab.

Lastly, I would like to thank my family and friends. Your support was invaluable in helping me get through the long nights and tough times the past two years.

December 7, 2021

ABSTRACT

PLASMA ELECTROLYTIC OXIDATION OF PURE TITANIUM

AT CONSTANT APPLIED VOLTAGE

Publication No. _____

Hunter Pitts; M.S.

The University of Texas at Arlington

Supervising Professor: Dr. Efstathios I. Meletis

Plasma Electrolytic Oxidation (PEO) is a method of coating which is used to apply non-metal coatings to different metal substrates. This process occurs in an electrochemical cell that consists of an electrolyte, two electrodes submerged in the electrolyte and a power supply supplying voltage to the two electrodes. The goal of this study was to observe how a constant applied voltage would affect the coating thickness at varied applied voltage and varied processing time.

This study was a continuation of a constant applied voltage study previously performed in the SaNEL research group. It was continued to add more detailed thickness data, develop a better understanding of the PEO process under constant voltage, and facilitate an undergoing

modeling effort in SaNEL by another group member. The electrolyte used in the present study was KOH and $K_4P_2O_7$, and the substrate pure Titanium (Ti) being the same as previous in experiments for continuity.

PEO is an anodic process, which requires the positive polarity to be attached to the Ti electrode and the negative polarity to be attached to the stainless-steel counter electrode. A programmable power supply was used to apply constant voltage to the Ti working electrode. Four different voltages (450, 400, 350 and 300 V) were applied to the Ti electrode at varying processing times for each voltage. For 450 V, the processing times of 2, 10, 20, 30, 50 ,70, 100 and 150 s were selected to get a good range of time across the whole PEO process. For 400, 350 and 300 V the processing times of 50 and 100 s were selected for each.

By applying a constant voltage to the Ti substrate, as the coating increases in thickness, the current decreases until it reaches zero. The current density can be calculated from the current decay data and the current density decays are compared across each voltage. As voltage increases the time for current density to decay to zero also increases, as well as the maximum current density value being higher at higher voltages. Surface morphology, composition, and thickness were characterized by SEM, SEM/EDS and XRD. EDS and XRD were used to confirm the presence of Ti, O and P in the coating and offer insight into which possible compounds are formed in the coating. It was determined that multiple Titanium oxides and amorphous Titanium phosphates are present in the coating, with TiO_2, Ti_2O and TiP_2O_7 being the most probable compounds found in the coating.

SEM was also used to obtain the coating cross section thickness. It was determined that as applied voltage increased the coating thickness also increased and the coating thickness can grow for longer times at higher applied voltage as well. The thickness values obtained for 450 V

were compared to a model made to predict oxide growth for the PEO process on Ti. The results of this comparison found that the thickness measurements obtained experimentally matched well with the model.

Finally, charge density calculations were conducted for each deposition and correlated to the thickness data. The charge density is found by taking the integral of the current density decay curve with respect to time. A plot of charge density versus thickness was made to show the relationship between the two. It was determined that the relationship between the two is linear and can help be used to predict the thickness based only on experimental data. If the current density decay curve is obtained experimentally and the charge density is calculated from this curve, the thickness can be in turn estimated. This could be a helpful tool to use alongside the oxide prediction model to help be more accurate in trying to predict potential oxide growth at specific PEO parameters.

TABLE OF CONTENTS

LIST OF FIGURES

Figure

LIST OF TABLES

Table

CHAPTER 1

INTRODUCTION

1.1 Introduction and Motivation

Titanium is an important material and is used in many fields such as computers, aerospace, automotive, biomedical, and other manufacturing fields. It is such a widely used material due to it having a high natural corrosion resistance, but one downside to using it is that it has a low wear resistance [1]. A common method to combat this low wear resistance is to apply so sort of coating to the Ti metal surface [2]. Applying a coating to the surface will help to increase the wear resistance and corrosion resistance [2,3]. The increase to corrosion resistance is not as great or as important as the increased wear resistance due to Ti having a high corrosion resistance already, but there is no detriment in having the corrosion resistance increase further as well. Applying a coating to the surface of the Ti allows for the Ti to be functionalized for uses that it could not be used for before applying a coating. For example, past research done in the SaNEL research lab by W. Boonrawd allowed for a coating applied on a Ti substrate to be used to facilitate bone growth on the surface of the coating [4].

There are many possible methods to apply coatings to Ti that have been used in research and industry before. Some example of coating methods includes Physical Vapor Deposition (PVD), Electrolytic Plasma Processing (EPP) which encompasses both Plasma Electrolytic Deposition (PED) and Plasma Electrolytic Oxidation (PEO), Ion Sputtering, Electrocyrstallization and sol-gel application just to name a few [1,5,6,7]. For this experiment PEO was chosen because it has been shown to greatly improve mechanical properties, has a high deposition rate and good adhesion with the substrate [5]. PEO has also been increasing in use as

a method to coat Ti and Ti alloys as a nonmetallic coating which has improved surface properties [8].

There has been past research performed by some past members in the SaNEL research group regarding the PEO process on pure Ti substrates. PEO process at constant current density studies were performed by Mortazavi [2,8] while PEO at constant voltage studies were performed by Twaddle [5]. In the constant current density experiments, the voltage increases as the coating gets thicker to apply the same current density throughout the whole experiment. In the constant voltage experiments the current density decreases over time as the voltage remains constant due to the coating getting thicker. The goal behind this research is to continue from what has been done in the constant voltage experiments previously. This will provide a better understanding of the PEO process, allow for more data to be used and compared with the previous data which will facilitate a modeling effort undergoing in the SaNEL lab group. The present detailed data and further understanding will assist in the theoretical prediction of oxide growth under various PEO processing parameters.

1.2 Research Objectives

The objectives of this research include:

- To continue constant voltage PEO experiments to improve our current understanding of the PEO process, conduct a series of well-defined experiments and obtain reliable data to assist in formulation of an Oxide Growth model.
- Assess the effect of voltage and processing time on coating thickness.

- Characterize the coating surface and cross section using SEM, EDS and XRD.
- Characterize and develop an understanding of the current density decay as a function of time at different voltages.
- Determine the relationship between oxide thickness and charge density applied to substrate.

CHAPTER 2

LITERATURE REVIEW

2.1 Plasma Electrolytic Deposition

Electrolytic Plasma Processing is an electrochemical process which requires a high electrical potential to operate [9]. The EPP system consists of a power supply, an electrolytic cell, an aqueous electrolyte and two electrodes [9]. EPP is a general term which overlaps both PED and PEO. If the working electrode, the electrode that you want to apply coating to, is connected to the negative output on the power supply the surface can be cleaned or metal film can be coated on the surface [9,10]. This process is known as PED, which is a cathodic process. However, if the positive output from the power supply is connected to the working electrode, then a layer of oxide can be formed on the substrate surface [9]. This process is known as PEO and unlike PED, PEO is an anodic process. An EPP treated surface, either PED or PEO, becomes rough and comprised of hills, valleys and pores of varying size based on processing parameters [9]. One of the benefits of the EPP process is that it is environmentally friendly and does not create any waste besides the electrolyte being used [11].

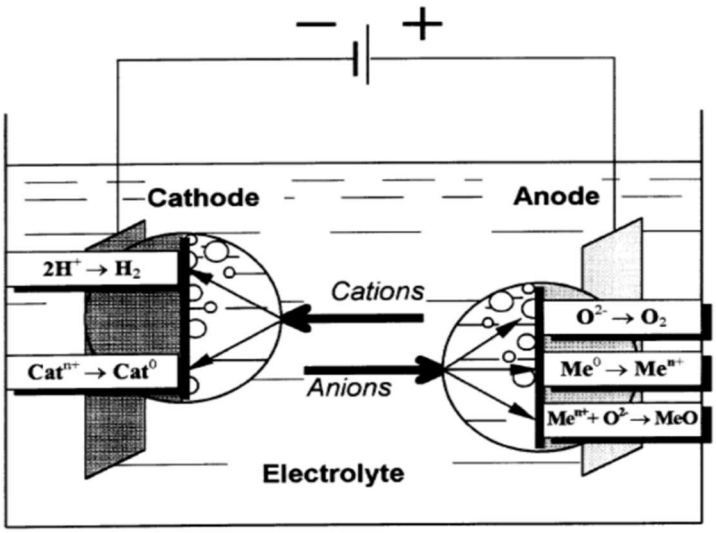

Figure 2.1: Image of a typical Electrochemical cell for the EPP process [9].

A general schematic for the PED mechanism is shown below in figure 2.1 [11]. Since PED is a cathodic process, the working electrode has a negative charge being applied to attract positive metal ions to the surface where the plasma begins to form. Due to high voltage the surface of the metal heats up and plasma bubbles begin to form, as seen in step a, figure 2.2. The plasma begins to expand in step b, and this causes a shock wave. As the plasma bubble collapses in step c, the force causes metal ions to get injected in the rapidly cooling plasma bubble. Step d, the plasma bubble bursts, and the metal ions become intertangled with the substrate to form a coating. The coating then rapidly cooled (quenched), and a metal coating is applied to the surface. As this process continues, it develops a rough layer due to the cycle of plasma bubbles forming and bursting at random locations across the surface of the substrate. Figure 2.2 shows the process as it pertains to PED but if the polarity of the working electrode is changed, Oxygen anions will be attracted to the surface instead. This process is the counterpart of PED, PEO, which has the same process as shown.

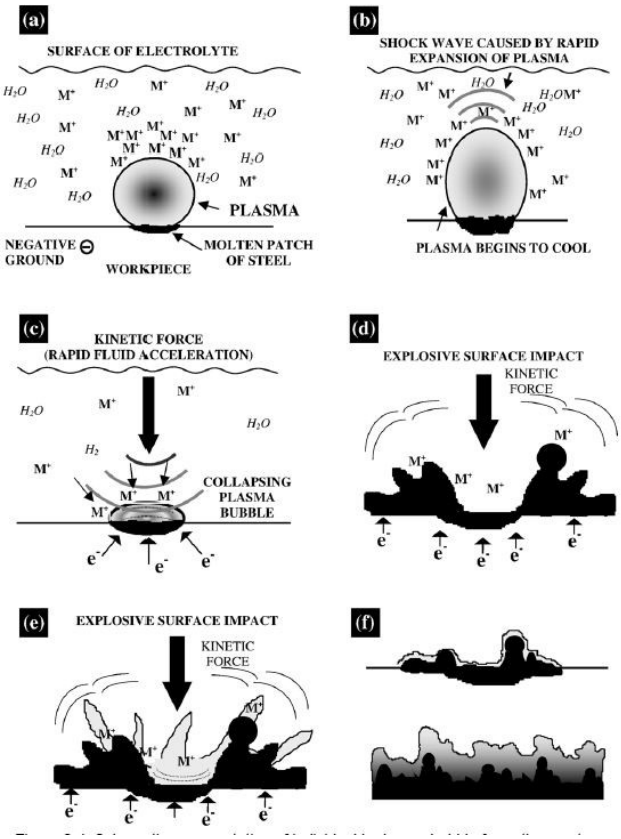

Figure 2.2: Schematic of PED mechanism [11].

2.2 Plasma Electrolytic Oxidation

The PEO process occurs when the positive source from the power supply is connected to the working electrode, which is an anodic process [9]. During the PEO process, a continuous layer of oxygen gas surrounds the surface of the working electrode [9]. The high voltage applied generates a highly localized electric field between the two electrodes [9]. The high voltage causes the surface temperature of the working electrode to rise as plasma is formed on the surface. These high temperature plasma discharges lead to localized melting of the substrate around these discharges, which forms discharge channels [9]. The discharge channels that form facilitate the oxygen transfer into the substrate followed by rapid cooling forming an oxide layer along the surface of the substrate.

The PEO process can be seen as a function of voltage increase in figure 2.3. As the voltage increases more plasma will be observed on the surface but below a certain voltage no plasma will appear on the surface. The minimum voltage at which plasma occurs on the surface is known as voltage breakdown [5]. Below this breakdown voltage, there is no plasma that forms on the surface, so the surface is not locally melted, and no coating is able to form. The opposite end of the spectrum is if the voltage is too high, which is known as the critical voltage. Above this critical voltage, the micro-discharges of plasma become more intense until ultimately arcing occurs on the surface, which in turn, can be damaging to the coating. Another example of the breakdown voltage can be seen in figure 2.4. This figure shows the PEO process at six different voltages. The lowest voltage image is the PEO process at 273 V and only shows gas bubbles. Increasing the voltage to 300 V, plasma can be observed on the surface. For this example, the breakdown voltage occurs somewhere between 273 V and 300 V. Similarly, as the voltage is increased, the frequency and size of plasma on the surface also increases, which can cause thicker coatings to grow, up until the critical voltage threshold.

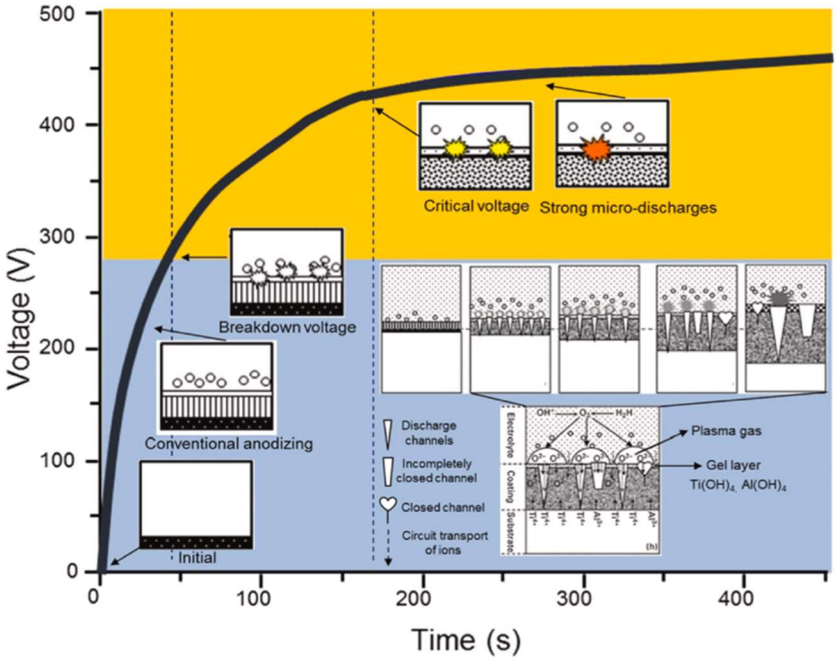

Figure 2.3: PEO process shown as voltage increases [9].

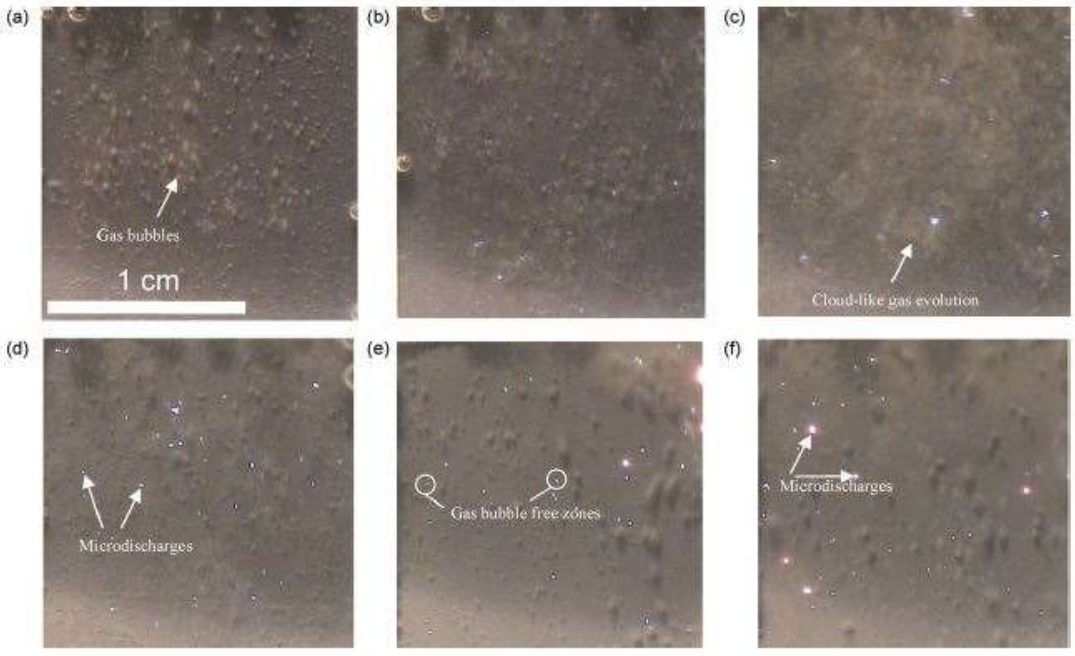

Figure 2.4: PEO Process at different voltages [12] (a. 273 V, b. 300 V, c. 350 V, d. 405 V, e. 430 V, f. 435 V)

Titanium is commonly used as a substrate for the PEO process because of the stable oxides that it forms. It has been determined that there are multiple oxide phases that can form between Ti and O, TiO_2 being the most common [13]. Due to the nature of the PEO process, a mixture of many oxides will most likely form. This is because PEO is a non-equilibrium process due to its rapid heating and rapid cooling of the coating surface on the substrate. The phase diagram shown for Ti and O is the equilibrium phase diagram, figure 2.5. Since PEO is a non-equilibrium process, the phase diagram can only be used as a baseline for possible oxides that can form during the PEO process on pure Ti.

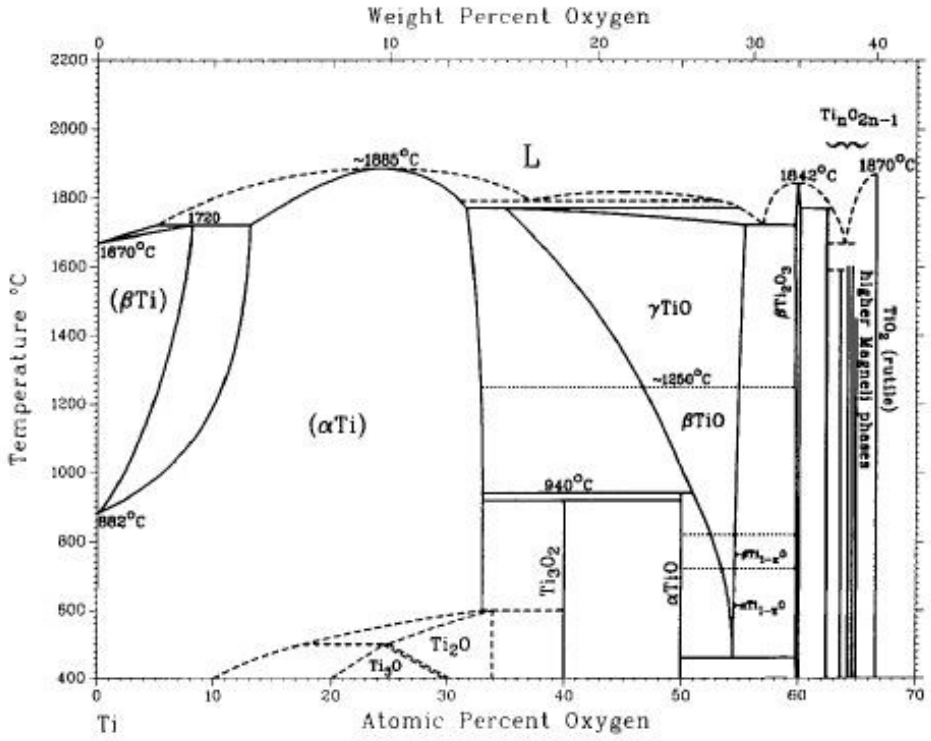

Figure 2.5: Equilibrium Ti-O phase diagram [13].

There are two types of currents that participate in the PEO process, the electronic current and the ionic current. The electronic current is responsible for the heating of the substrate while the ionic current is the one responsible for oxide growth on the substrate. Figure 2.6 shows the difference between the total current density (in blue) and the ionic current density (in red). By subtracting the two, the electronic current density can also be determined.

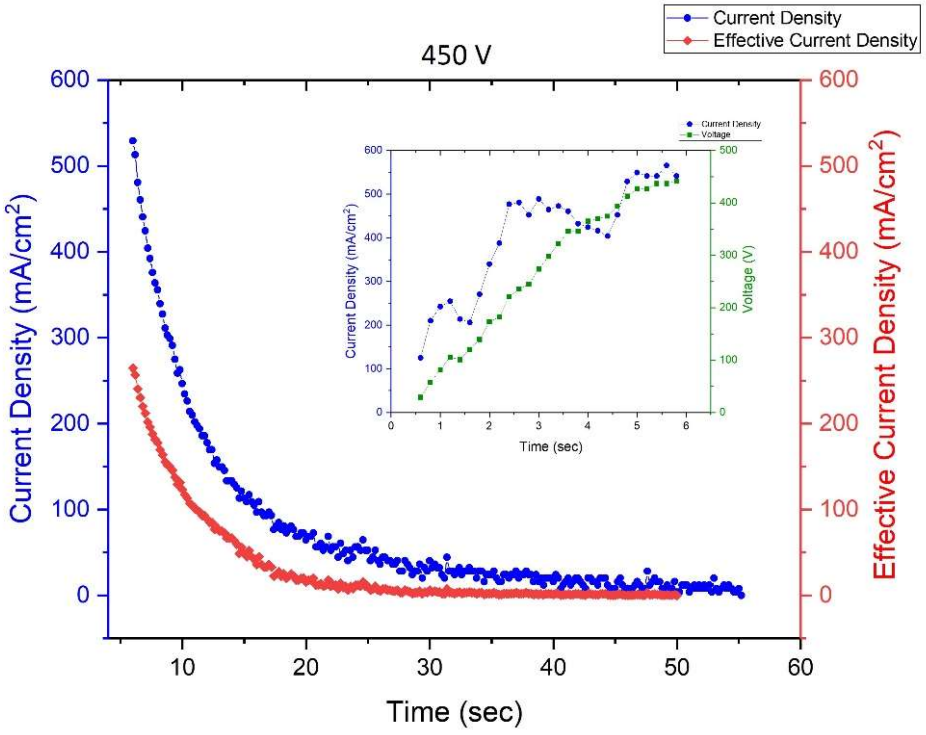

Figure 2.6: Current Density Decay During PEO process on pure Ti at 450 V [5].

Different electrolytes can be used in the PEO process to form oxides on the surface of the substrate. First, Jung et al. [14] studied the effect of different electrolytes on PEO of Ti. In this study, it was determined that having Potassium ions in the electrolyte can help to increase the thickness of the coating. Therefore, KOH was chosen to be used in the electrolyte. A study was performed in Shokouhfar at al. [15] of varied electrolytes to determine which electrolyte offers the best corrosion resistance. In this study it was determined that electrolytes containing

Phosphorous offered the best corrosion resistance, which was the basis for choosing $K_4P_2O_7$ being used in the present experiments.

CHAPTER 3

EXPERIMENTAL STUDY

3.1 Materials and Electrolyte

The metal substrate used in this experimental study was pure Titanium strips of 0.5 mm thickness. A hole was drilled in the strip to apply voltage via an electrode and then, insulated to selectively apply voltage to a specific surface area, figure 3.1. Each strip was insulated by using heat shrink wrap around all the sides only leaving the working area of the electrode exposed to apply coating to, figure 3.2. The surface area used for all experiments was 2.15 cm^2.

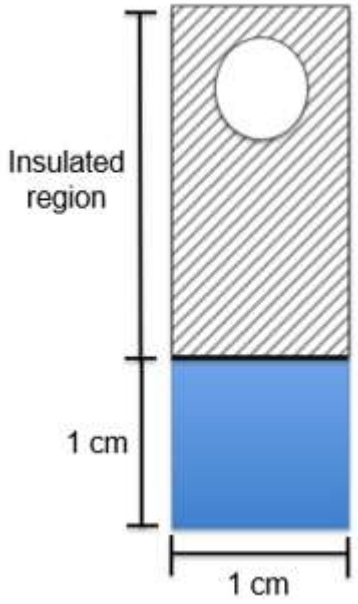

Figure 3.1: Schematic of sample used in experiments

Figure 3.2: Example of insulated sample connected to electrode before processing

Since the PEO process requires an electrochemical cell to be formed, an electrolyte needs to be used. A mixture of Potassium Hydroxide (KOH) and ($K_4P_2O_7$) in Deionized (DI) water were used as the electrolyte. This was chosen because this is the electrolyte used in previous PEO experiments in the SaNEL lab and prevent the addition of another new variable to the experimental process. To prepare the electrolyte 0.0173 g of KOH pellets and 0.9911 g of $K_4P_2O_7$ powder were added to 300 mL of DI water which gives concentrations of 0.001 M KOH and 0.01 M $K_4P_2O_7$. The pH and conductivity of the electrolyte used was measured by a pH meter and conductivity probe before and after each processing experiment. The average starting pH across all experiments was 11.23 and the average starting conductivity across all experiments was 4.11 mS.

3.2 Processing Procedure

The insulated sample shown in figure 3.2 was attached into a double walled beaker using a rubber stopper to hold it in place. A stainless-steel counter electrode was used, which wrapped around most of the inside of the beaker, figure 3.3. 300 mL of electrolyte was placed in this

setup as well as a stir-bar. Water was flown through the outer portion of the double walled beaker to apply cooling. Since PEO is an anodic process, the positive electrode is attached to the working electrode (pure titanium sample) and the negative electrode is attached to the counter electrode (stainless steel). This is done by using alligator clips coming from the positive and negative ports on the power supply used. The power supply utilized for this process was an Ametek SGX 660/33 programable power supply.

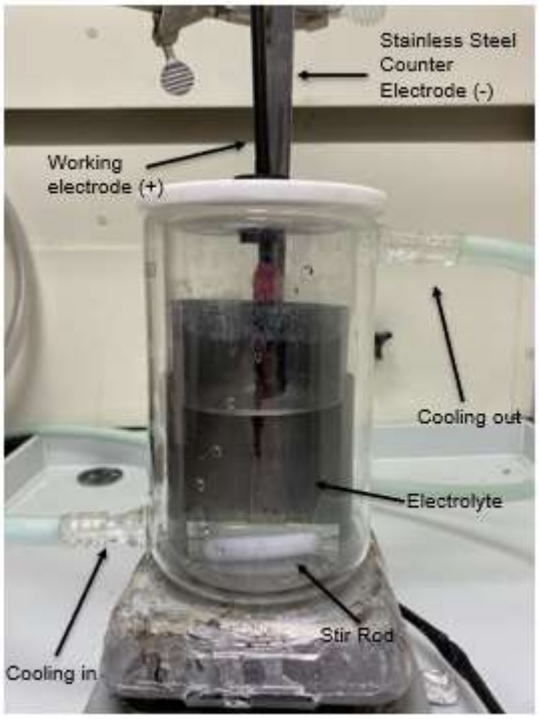

Figure 3.3: Experimental setup used for PEO process

The power supply used is programmable so the whole coating process where voltage and current are applied is completely done using an application on a connected computer. Since this experiment was conducted at constant voltage, the constant voltage mode was selected on the power supply. Once that has been selected, the sequence of events can be edited in the sequence editor feature on the power supply. First is applying voltage from 0 V to whatever maximum

voltage is selected. Through many experiments and trial and error it was found that increasing from 0 V to 450 V in 2 s was the best voltage increase rate for the experiment. Next, the voltage was held constant at the selected maximum applied voltage. Finally, the applied voltage was decreased to 0 V in 1 s. An example of this process is shown below in figure 3.4. After turning off the applied voltage, live voltage mode can be turned off, so it is safe to touch the electrodes. The titanium substrate is taken out and sheared off the rest of the sample in the insulated region so that the surface area that was coated can be analyzed. Lastly, the electrolyte is tested for pH and conductivity after the process is completed.

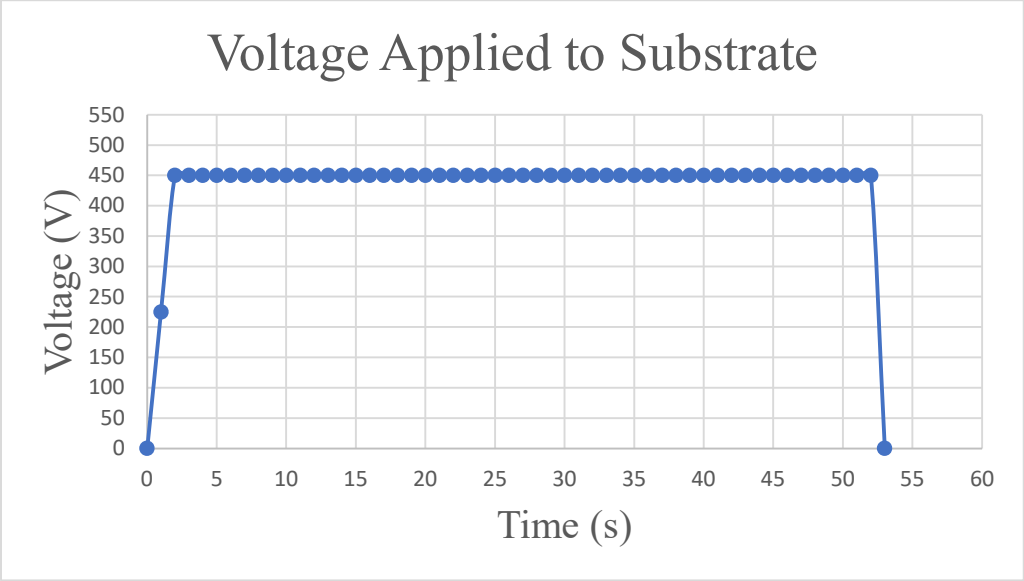

Figure 3.4: Example of applied voltage – time cycle experiment.

To collect the voltage and current vs time data, a Tektronix tds2001C oscilloscope was used . This data was utilized to obtain the current density decay as well as the charge density data with time for each experiment.

Four different voltages were chosen for the constant voltage experiments, 450 V, 400 V, 350 V and 300 V. The reason for this selection was to make sure that the breakdown voltage of Titanium, which is 275 V, was reached by each voltage. For all four voltages selected, PEO experiments for 50 s and 100 s were performed, as well as 150 s, 70 s, 30 s, 20 s, 10 s and 2 s for 450 V, Table 3.1. The reason for selecting more processing periods for 450 V was that the current decay for that voltage lasted much longer compared to the lower voltages.

Table 3.1: Voltages and times for each PEO experiment performed.

Experimental Tests	
Voltage (V)	Experimental Time (s)
450	150, 100, 70, 50, 30, 20, 10, 2
400	100, 50
350	100, 50
300	100, 50

3.3 Characterization Procedure

3.3.1 Current Density and Charge Density

Once the Current vs Time data has been obtained from the oscilloscope, the current density decay was obtained and plotted vs time. To obtain the charge density data, the integral is taken of the Current Density decay data to find the area under the curve, which is equivalent to the Charge Density.

3.3.2 SEM and EDS

The surface morphology and cross sections of the samples were analyzed by Secondary Electron Microscopy (SEM). A Hitachi S-3000N SEM was used for all SEM and EDS shown in the results and discussion section. The accelerating voltage used was 25 kV and the working distance around 15 mm. These micrographs and analysis were used to help identify the coating composition visualize the roughness and porosity of the coating and to obtain the coating thickness for each of the times specified, besides 450 V 2 s.

3.3.3 XRD

XRD (X-ray Diffraction) was used for 3 different samples to help determine phases present in the coating. XRD was performed using the Bruker D8 X-ray Diffractometer. Each sample was analyzed using the Θ-2Θ mode from 20-80°. For each analysis, an accelerating current of 40 mA and a voltage of 40 kV. An increment of 0.01° with a scan speed of 1 sec/step was used to obtain high accuracy for each diffraction. Finally, all three spectra are aligned over one another to align the peaks with one another to analyze the peaks more easily.

3.3.4 Mounting and Polishing for Cross Sections

After the data for surface of the coating was obtained, cross sections of samples were prepared to determine coating thickness. First, the samples were cut in half using a low-speed diamond saw cooled with water. Once the sample has been cut, it was mounted in Bakelite. To make sure the sample stays upright during the mounting process, a stainless-steel spring is used to hold the sample vertical.

Between 10-12 mL of Bakelite was used for each sample in the hot-press. The Bakelite and sample were heated for 10 minutes under pressure in the hot-press and then cooled for 10 minutes under pressure as well. After mounting, the sample were ready to be polished.

Polishing was done using a stationary disc that circular sandpaper could be applied to at different grit size. The side of the mounted sample with the exposed cross-section was polished using increasing smoothness of sandpaper up to 1000 grit. The grits used were 120, 180, 240, 320, 400, 600, 800 and lastly 1000 grit. Subsequently, a fabric pad with alumina powder dissolved in water was used to polish the cross-section finer. Three different sizes of alumina were used 1 μm, 0.3 μm and lastly 0.05 μm. A 3:1 mixture of alumina to water was used for each of the different sizes of alumina used.

CHAPTER 4

RESULTS AND DISCUSSION

4.1 Current Density Decay

PEO experiments were conducted at different voltages and processing time to allow determination of coating growth characteristics. Figures 4.1-4.4 present the current density decay as a function of time for various applied voltages. A consistent current density decay trend is observed for each applied voltage. As expected, the level of current density observed depends on the applied voltage with higher voltages achieving higher current densities. Thus, the maximum current density observed for 450 V, 400 V, 350 V and 300 V is 1200 mA/cm^2, 1000 mA/cm^2, 700 mA/cm^2 and 600 mA/cm^2, respectively. This means a larger current is flowing through the same size surface area at higher voltage and should produce a thicker coating as a result. Also,

the time it takes for the current density to decay to zero is longer at higher voltage. For 450 V this time is around 50 s, 400 V around 30-35 s, 350 V around 20 s and 300 V around 10 s. This means that since the current density dies out, no additional coating formation should occur by prolonging the processing time. The difference in maximum current density and decay time can be clearly demonstrated in figure 4.5. In addition, the graph also shows that a higher voltage produces a larger area under the current density vs time decay curve. This means that at higher voltages, the total charge density supplied to the sample is also higher. This again can help to support that at a higher voltage a thicker coating can be produced for the same processing time.

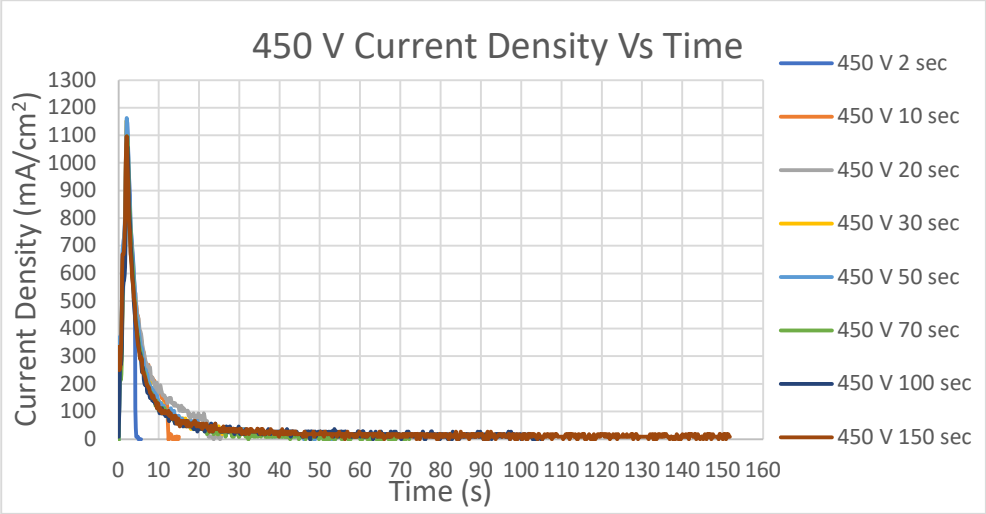

Figure 4.1: Current Density Decay for 450 V as a function of processing time.

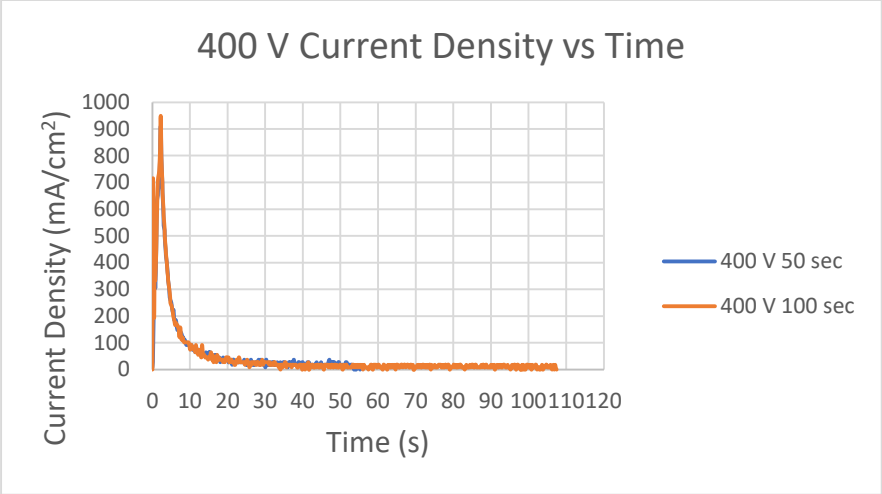

Figure 4.2: Current Density Decay for 400 V as a function of processing time.

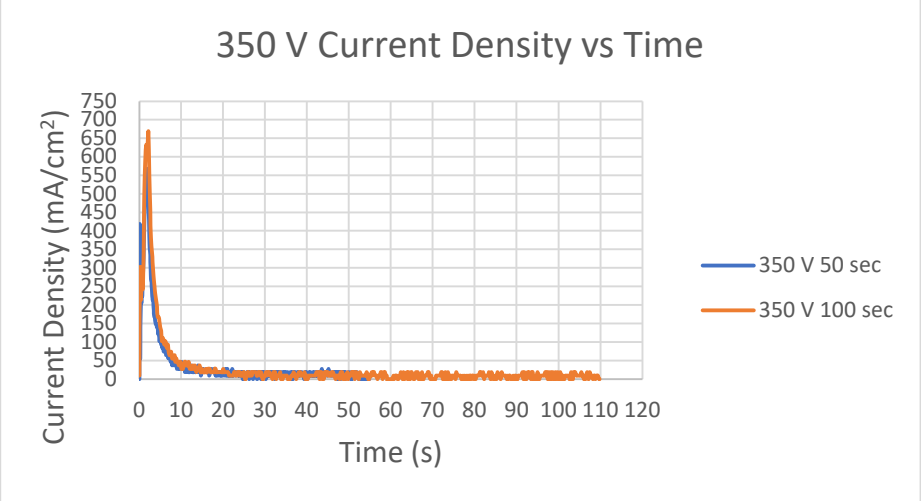

Figure 4.3: Current Density Decay for 350 V as a function of processing time.

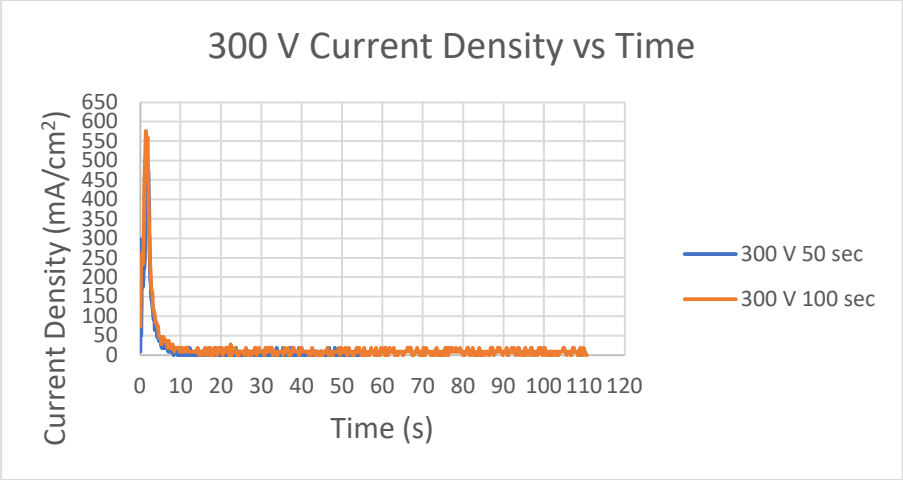

Figure 4.4: Current Density Decay for 300 V as a function of time.

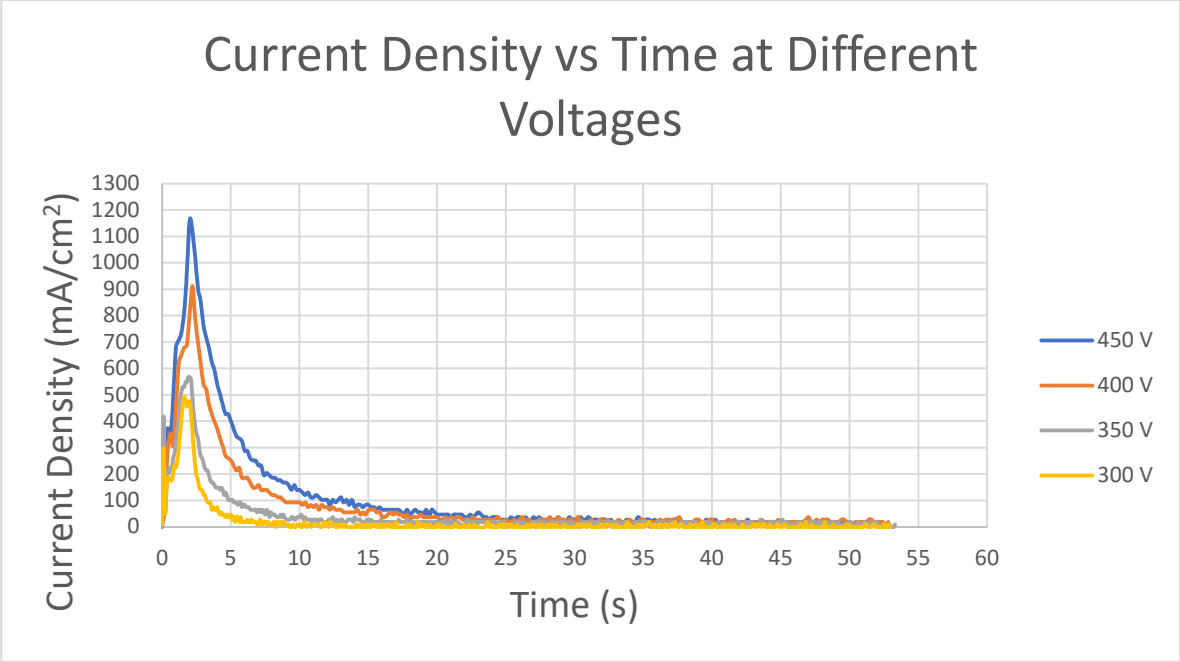

Figure 4.5: Current Density decay for 50 s for all four voltages applied in the PEO process

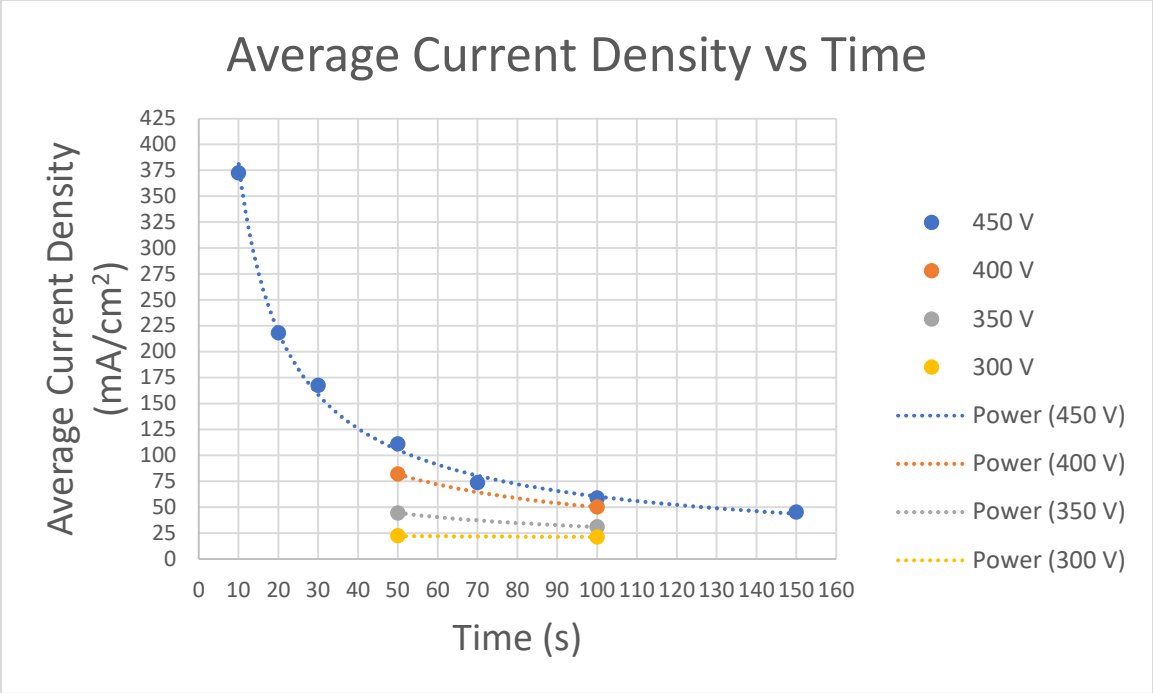

Figure 4.6: Average Current Density as a function of voltage

The average value of the current density was calculated for each applied voltage and is presented in fig. 4.6. The graph clearly demonstrates that PEO processing at 450 V can keep the coating process active for longer time while for low voltages (350 V and 300 V) dies out very fast. As seen in the graph, processing at 300 V for 50 to 100 s the current density is basically flat and thus, lacks any potential to cause coating growth. The present results show that only high voltage processing has the potential to increase coating thickness with increasing the processing time.

4.2 SEM and SEM/EDS

The surface composition and morphology were characterized before examining the cross sections for each sample. An inherent characteristic of the PEO process is discharge channel

formation resulting in porosity and surface roughness. As processing time increases a large number of pores are expected to be produced. For example, the pores in the 450 V 2 s sample shown in figure 4.7 are smaller than the ones in the 450 V 10 s sample in figure 4.8. The difference in roughness and pore size is hard to distinguish just from examining the 2 s and 10 s samples. Figure 4.9 shows the 450 V 100 s sample and based on the image, the pores and roughness are greater than in the latter two samples processed at shorter time. As the time increases the pores and roughness would also increase. Similarly, looking at the sample composition from the EDS analysis, it is evident that the composition of the coating also changes over time. In the 450 V 2 s and the 450 V 10 s samples the atomic percent of Oxygen is relatively high at 59.33% and 57.1% respectively. The atomic percent Oxygen in the 450 V 100 s sample is significantly lower at 37.99%. Just as there is less Oxygen present over time there is more Titanium present over time. This is shown by the increasing atomic percent from 37.34%, 38.63% and 55.68% for the 450 V 2 s, 10 s and 100 s samples, respectively. Another element present in the coating is Phosphorous. Phosphorous is present due to the use of $K_4P_2O_7$ in the electrolyte. The Phosphorous content is significantly less than the other two elements present, but it still slowly increases in percentage as time increases. These percentages are 3.33% for the 2 s sample, 4.27 % for the 10 s sample and 6.33% for the 100 s sample. However, it should be noted that RDS analysis from the sample surface is only indicative of the composition. It can't provide reliable composition data since it is produced from a larger volume below the sample surface.

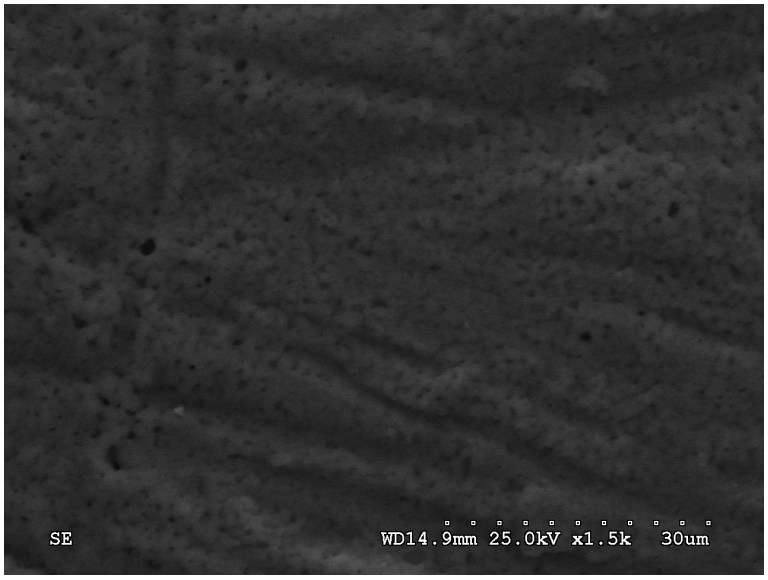

Figure 4.7: SEM micrograph of the surface of the coating processed at 450 V 2 s.

Table 4.1: EDS compositional analysis of the sample shown in figure 4.7

Atom	**Atomic %**
Oxygen	59.33
Phosphorous	3.33
Titanium	37.34

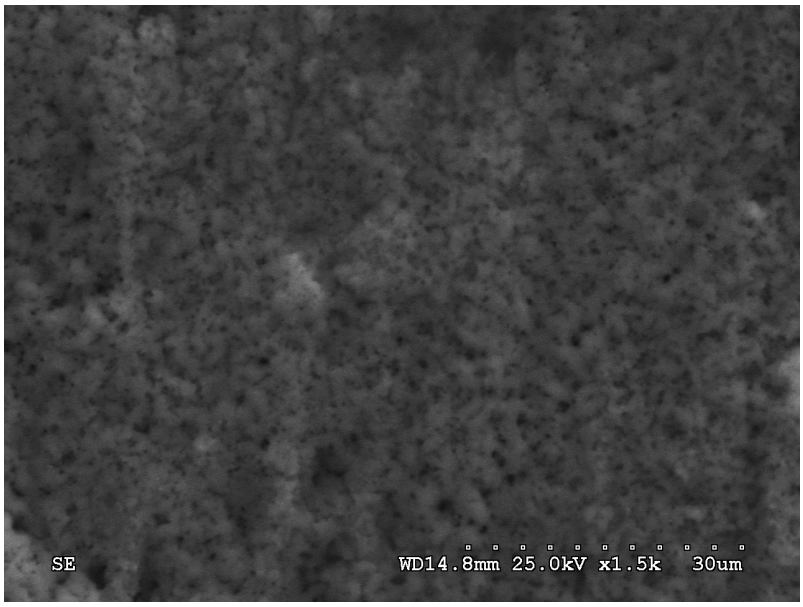

Figure 4.8: SEM micrograph of the surface of the coating processed at 450 V 10 s.

Table 4.2: EDS compositional analysis of the sample shown in figure 4.8

Atom	**Atomic %**
Oxygen	57.1
Phosphorous	4.27
Titanium	38.63

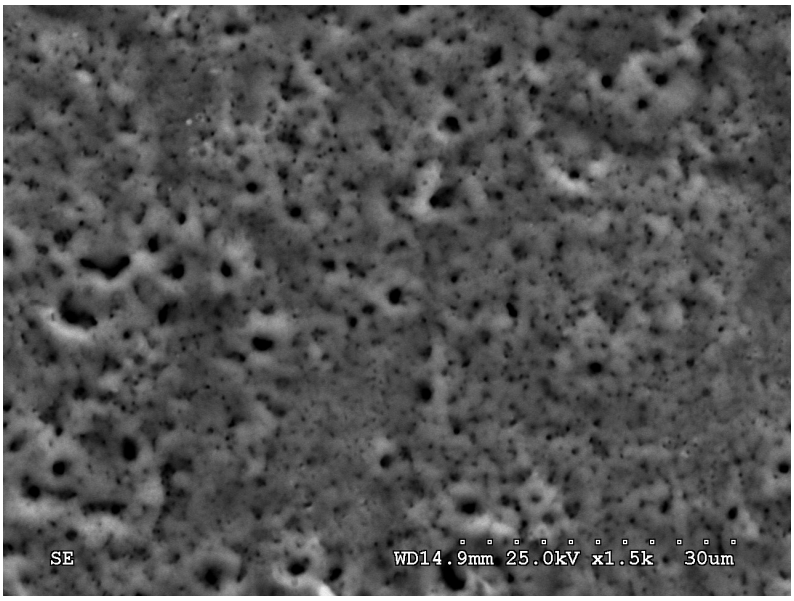

Figure 4.9: SEM micrograph of the surface of the coating processed at 450 V 100 s.

Table 4.3: EDS compositional analysis of the sample shown in figure 4.9

Atom	Atomic %
Oxygen	37.99
Phosphorous	6.33
Titanium	55.68

Following EDS analysis of the sample surface, EDS analysis was conducted on the cross-section of the coatings. To obtain a cross-section, the samples were mounted in Bakelite and polished as described earlier. A typical coating cross section is shown in the SEM image in figure 4.10.

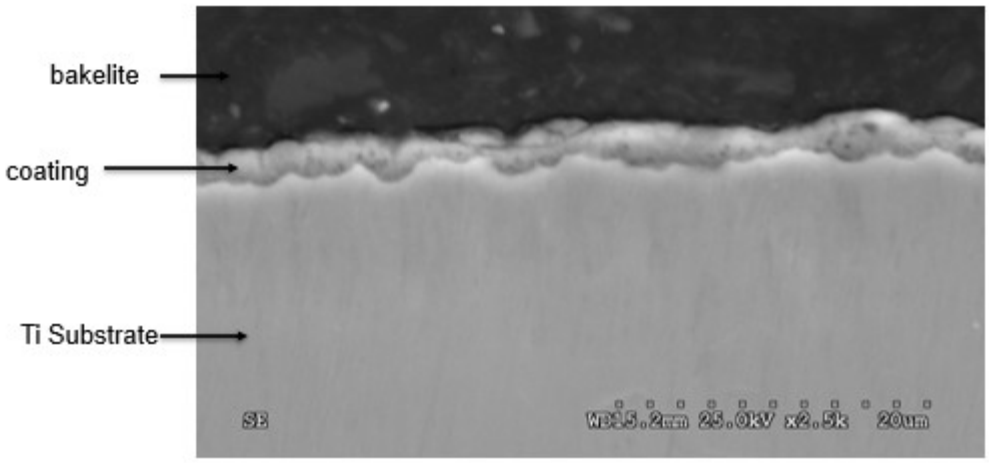

Figure 4.10: SEM micrograph of coating cross section (450 V 50 s).

An EDS line scan was performed on the cross section to determine how far the coating extends and the thickness of the "mixing region" region between the substrate and the coating. Figure 4.10 shows the top coating while the lighter layer just below it is the mixing region. From the line scan taken at the location specified in figure 4.11, the coating is about 3 μm thick while the mixing regions is about 1 to 1.5 μm thick, figure 4.12. It is clear from the composition profile that the mixing region has a gradient O content from 0 to 50 at.% O. On the other hand, the coating composition has an O content from 50 at.% to more than 75 at% O as the surface is approached, while some P is also present. This composition analysis suggests that several different Ti oxides might be present in the coating starting from TiO to TiO_2. However, since the coating in not uniform, as can be clearly seen in the micrograph, the coating exhibits a variation in thicknesses at different locations.

Something to note is the difference in the atomic composition compared to the surface EDS analysis. From the graph shown in figure 4.12 the Oxygen content is a lot higher in the coating, around 75 % as compared to the EDS of the surface of the coating. The line scan was

performed on the 450 V 100 s sample. That is the reason it was important to conduct EDS of both the cross section and the surface of the coating. Using EDS spot analysis can even further help to understand what is going on in the coating and that will be investigated next.

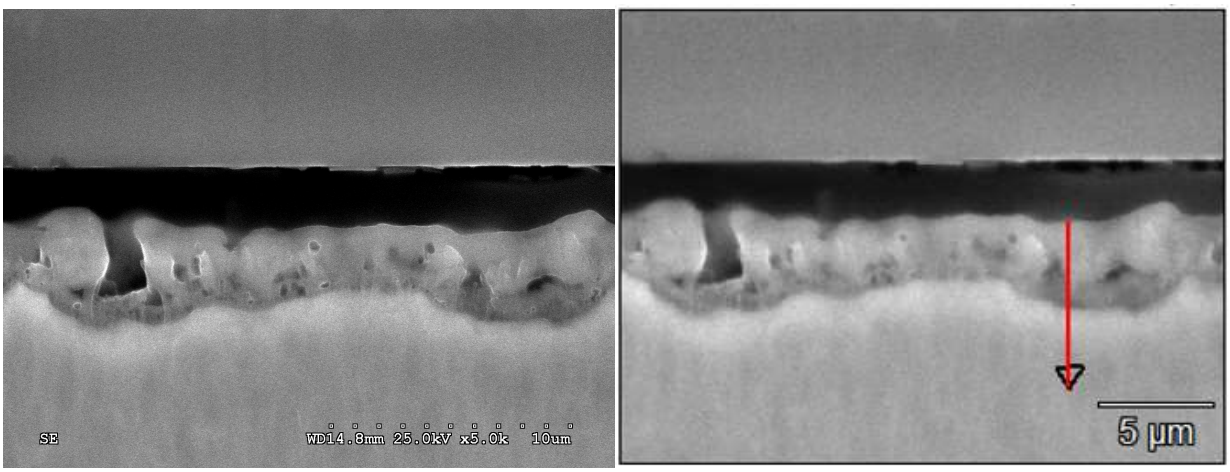

Figure 4.11: SEM micrograph used for EDS line scan (450 V 100 s).

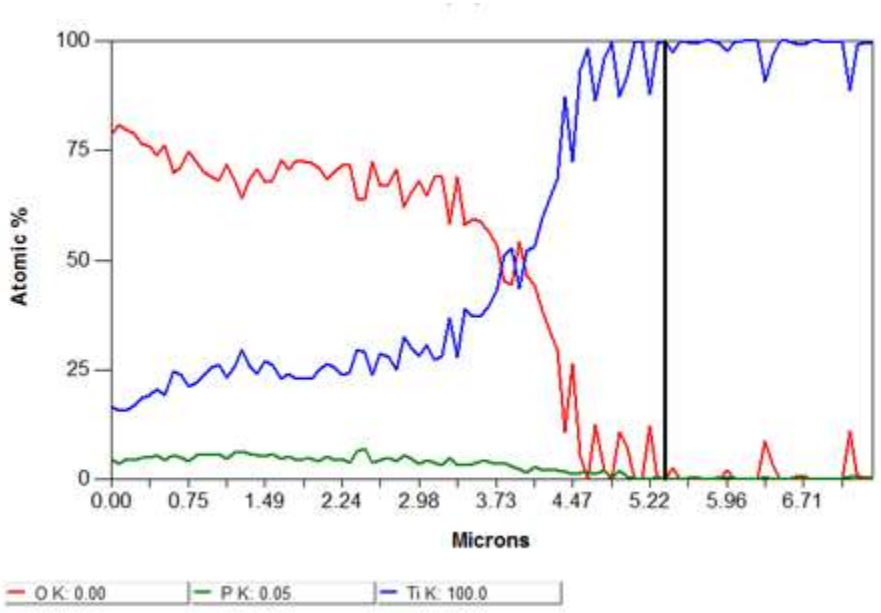

Figure 4.12: EDS line scan data obtained from the sample shown in figure 4.11

EDS spot analysis was also performed to help better define the atomic composition of the coating. The 450 V 100 s sample was selected for the spot analysis. Point 3 is the spot farthest away from the substrate in the coating and has also the highest atomic percent Oxygen at 55.16%. The next spot is point 2 and it has the next highest atomic percent Oxygen at 51.17%. Point 6, which looks to be at the edge of the coating and mixing region still has an atomic percent of oxygen of 25.18%. Then, in descending order of atomic percent oxygen, point 1 at 16.55%, point 5 at 13.41 % and finally point 4 with 7.93%. The latter points belong to the transient zone produced by Oxygen diffusion into the Ti substrate.

The results in figure 4.12 provide a clear picture of the Oxygen variation in the coating as a function of the distance from the coating surface. Oxygen content is apparently higher as the surface is approached since it is provided by the PEO oxidation process at the surface.

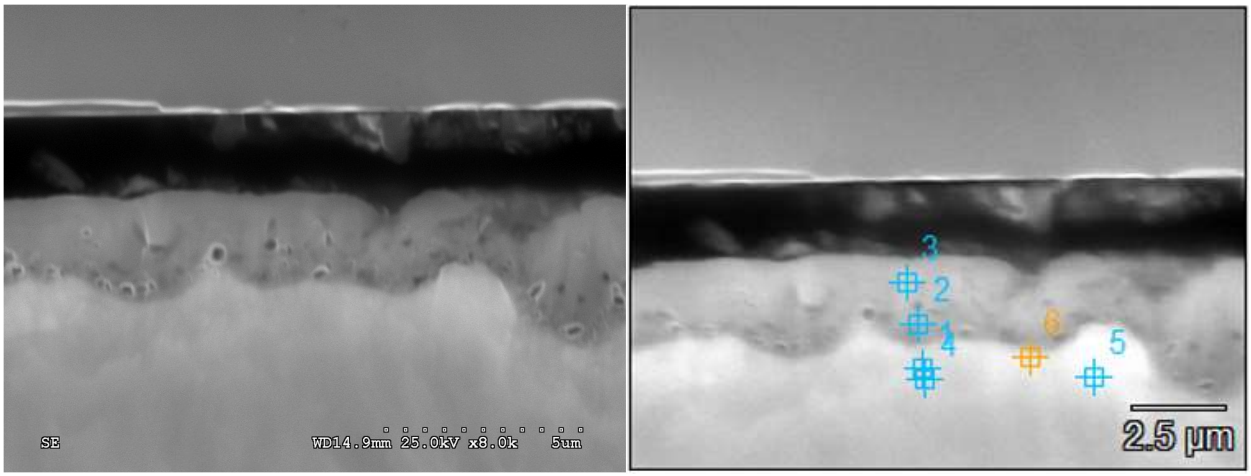

Figure 4.13: SEM micrograph used for EDS spot analysis (450 V 100 s).

Table 4.4: EDS compositional analysis obtained from spot analysis shown in figure 4.13.

	O-K	Si-K	P-K	Ti-K
Base(10)_pt1	16.55	1.15	1.22	81.08
Base(10)_pt2	51.17	4.05	4.36	40.41
Base(10)_pt3	55.16	12.58	6.65	25.61
Base(10)_pt4	7.93	0.96	0.86	90.24
Base(10)_pt5	13.41	1.14	1.02	84.42
Base(10)_pt6	25.18	2.65	2.09	70.08

4.3 XRD Analysis

X-ray Diffraction patterns were obtained for the 450 V 2 s, 10 s and 100 s samples. These patterns for samples processed at three different times are compared to the expected d-spacings of pure titanium as shown in figure 4.14. The XRD results clearly show a complex diffraction pattern with several overlapping reflections. The first peak on the spectra has a d-spacing of 3.50 Å and it is surrounded by a broad reflection (up to $2\theta = 30^{o}$) of an amorphous phase. This peak is most likely from cubic TiP_2O_7 and other amorphous phases including Phosphorous as well as tetragonal TiO_2. It is interesting that this actual diffraction appears only in the sample processed for 100 s. This can be attributed to longer exposure of the sample at high temperatures that caused some crystallization of the amorphous phase. The second peak at 2.54 Å can be due to a mixture of TiO_2 and Ti_2O oxides. The next three peaks at 2.34, 2.24 and 1.73 Å are close to diffractions from Ti_2O and other Ti_xO oxides. The peak located at 1.47 Å is due to TiO_2. The second to last peak at 1.33 Å is again present due to Ti_xO oxides and the final peak of the spectra at 1.25 Å is due to the TiP_2O_7. Based on the XRD results, several forms of Titanium Oxide have been produced as well as amorphous Titanium Phosphate phases. Since many of these peaks overlap with one another it is hard to determine with confidence which Oxides are present. The most common compounds formed in the coating are likely TiO_2, Ti_2O and TiP_2O_7.

To figure out the exact phases of the oxides formed more research needs to be done, but this confirms the presence of the Titanium Oxides and Titanium Phosphates in the coating.

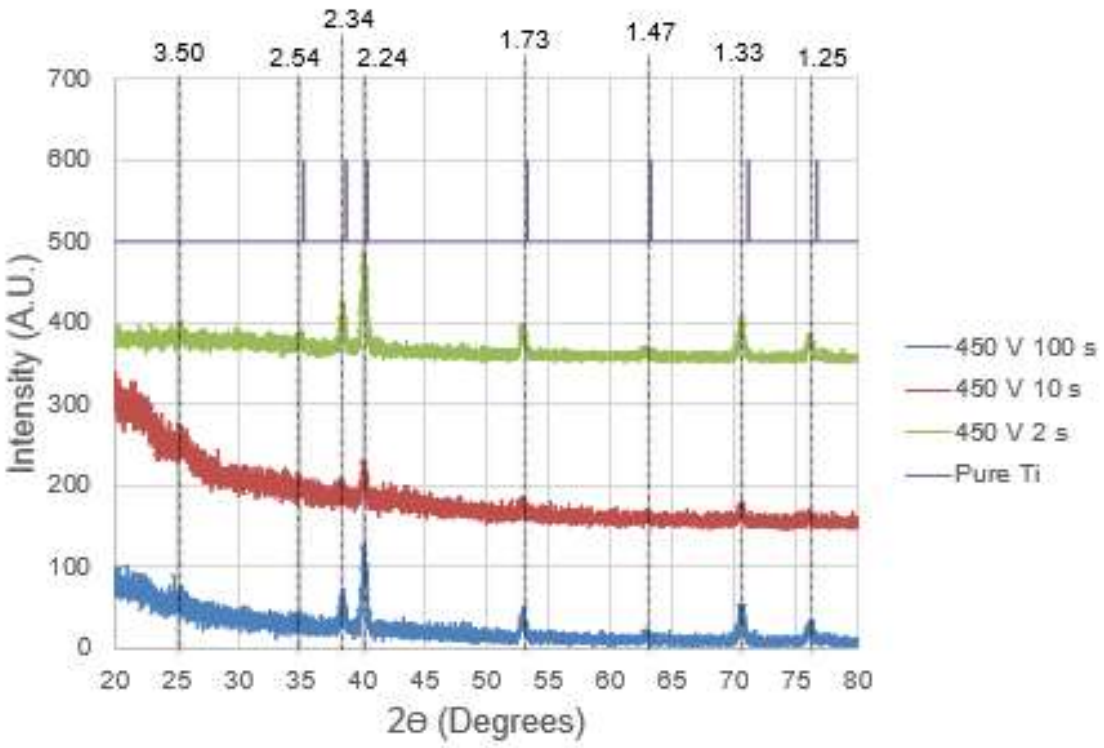

Figure 4.14: XRD spectra for 450 V 2 s, 10 s and 100 s compared with the location of known pure Titanium (hexagonal) peaks.

Table 4.5: Experimental d-spacing from 450 V data

Experimental Values	
Angle 2θ	d(Å)
25.2	3.5
35.02	2.54
38.31	2.34
40.2	2.24
53.08	1.73
63.52	1.47
70.51	1.33
76.29	1.25

Table 4.6: Pure Titanium peak data obtained from CCMB database.

Pure Ti hexagonal		
Angle 2θ	d(Å)	(h k l)
35.262	2.5432	(1 0 0)
38.68	2.326	(0 0 2)
40.387	2.2315	(1 0 1)
53.332	1.7164	(1 0 2)
63.284	1.4683	(1 1 0)
71.156	1.324	(1 0 3)
76.69	1.2416	(1 1 2)

Table 4.7: Ti_2O peak data obtained from CCMB database.

Potential Values Ti_2O (hexagonal)						
Angle 2θ	d(Å)	I%(f)	(h k l)	θ(°)	1/(2d)	2π/d
35.477	2.5283	8.9	(1 0 0)	17.738	0.1978	2.4852
38.159	2.3565	14	(0 0 2)	19.08	0.2122	2.6663
40.454	2.2279	100	(1 0 1)	20.227	0.2244	2.8202
53.084	1.7238	25.5	(0 1 2)	26.542	0.2901	3.6449
63.701	1.4597	18.4	(1 1 0)	31.851	0.3425	4.3044
70.517	1.3344	11.3	(1 0 3)	35.259	0.3747	4.7087
76.741	1.2409	9.8	(1 1 2)	38.371	0.4029	5.0633

Table 4.8: TiO_2 peak data obtained from CCMB database.

Potential Values TiO_2 (tetragonal)						
Angle 2θ	d(Å)	I%(f)	(h k l)	θ(°)	1/(2d)	2π/d
25.685	3.4655	100	(1 0 1)	12.843	0.1443	1.8131
38.396	2.3425	16	(0 0 4)	19.198	0.2134	2.6823
63.136	1.4714	2.5	(2 1 3)	31.568	0.3398	4.2702

Table 4.9: TiP_2O_7 peak data obtained from CCMB database.

Potential Values TiP_2O_7 (cubic)						
Angle 2θ	d(Å)	I%(f)	(h k l)	θ(°)	1/(2d)	2π/d
25.367	3.5082	85.2	(6 3 0)	12.684	0.1425	1.791
35.972	2.4946	1.4	(2 6 7)	17.986	0.2004	2.5187
38.409	2.3417	0.8	(2 4 9)	19.205	0.2135	2.6831
53.485	1.7118	4.9	(12,6,3)	26.742	0.2921	3.6704
63.847	1.4567	3.1	(6,9,12)	31.924	0.3432	4.3132
76.783	1.2404	0.6	(0,6,18)	38.391	0.4031	5.0657

4.4 Thickness Measurements

Based on the data shown so far, it can be determined that the coating is not uniform and has high roughness. This can be a problem in measuring the thickness of the coating as taking a measurement or a couple of measurements at a single point along the coating will not give an accurate coating thickness across the whole sample. A method for taking thickness measurements was devised to determine the thickness for each cross section at each different processing time and voltage. Since the length of the sample was 1 cm, it can be broken up into 10 equal lengths of 0.1 cm each. At each 0.1 cm, a SEM image can be taken and 10

measurements of equal distance along this piece of the cross section can be made. These measurements can be performed by using the measurement tool when viewing images on the SEM. This experimental procedure was followed to obtain reliable coating thickness data from all samples. Each SEM image was taken at 8000x magnification, accelerating voltage of 25.0 kV and a working distance of approximately 15 mm to keep each measurement as uniform as possible. If a SEM image is taken as close to every 0.1 cm as possible, there will be 10 measurements per image for a total of 100 measurements. Taking an average of these 100 measurements to give a more accurate measurement for coating thickness across the whole surface as well as the standard deviation for the measurements.

The thickness measurements for samples processed at 450 V follow a general trend of increasing with increasing processing time. It should also be noted that the standard deviation increases with increasing processing time as well. This is supported but the SEM images shown in figures 4.7, 4.8 and 4.9, which show higher porosity (and roughness) with increasing processing time. The average thickness measurements for 450 V are 1.97, 2.01, 2.16, 2.24, 2.49, 2.42 and 2.73 μm for times 10, 20, 30, 50, 70, 100 and 150 s, respectively.

Coating thickness for samples processed at 400 V also follows the trend of increasing thickness with processing time. The maximum thickness of 1.74 μm at 100 s of processing time still does not reach the lowest thickness of 1.97 μm in the 450 V 10 s sample. Again, coating thickness for samples processed at 400 V, the standard deviation increases as coating processing time increases. Coating thickness for samples processed at 350 V and 300 V also follow the same trends as found in the 400 V and 450 V but the standard deviation is much smaller. The processing time increases thickness as well as increases standard deviation but there is no overlap of thickness as the voltage increases. The minimum thickness value for 450 V is larger

than the maximum thickness value for 400 V which holds true for 350 V and 300 V as well. All the thickness values and their respective standard deviations are presented in tables 4.10 – 4.13.

-

Table 4.10: Thickness Measurements for Samples Processed at 450 V.

450 V		
Time (s)	Thickness (µm)	Standard Deviation (µm)
10	1.97	0.34
20	2.01	0.29
30	2.16	0.33
50	2.24	0.29
70	2.49	0.42
100	2.42	0.4
150	2.73	0.49

Table 4.11: Thickness Measurements for Samples processed at 400 V.

400 V		
Time (s)	Thickness (µm)	Standard Deviation (µm)
50	1.4	0.19
100	1.74	0.31

Table 4.12: Thickness Measurements for Samples Processed at 350 V.

350 V		
Time (s)	Thickness (µm)	Standard Deviation (µm)
50	1.01	0.15
100	1.27	0.2

Table 4.13: Thickness Measurements for Samples Processed at 300 V.

300 V		
Time (s)	Thickness (μm)	Standard Deviation (μm)
50	0.728	0.16
100	0.9	0.22

One of the main purposes of this research was to provide experimental measurements and compare them to an oxide growth prediction model. This model was produced by PhD student in SaNEL group, Kingsley Ochiabuto. Figure 4.15 presents the present experimental measurements and the model predictions. Comparing the model with the experimental thickness values the two are aligned well. The model was only made up to 100 s so the 150 s point is not shown but if the trend of the model continues the thickness value should align with the model. The only point that needs any explanation is the 450 V 10 s point. It is somewhat higher (even though within the standard deviation) than the model prediction. That can be explained by looking at the current density decay data. At low processing time the current density stays higher for the majority of the time with minimal decay. This suggests that at the few seconds in the beginning of the coating process, the majority of the coating thickness takes place, resulting in a disproportionally higher thickness compared to the rest of the samples.

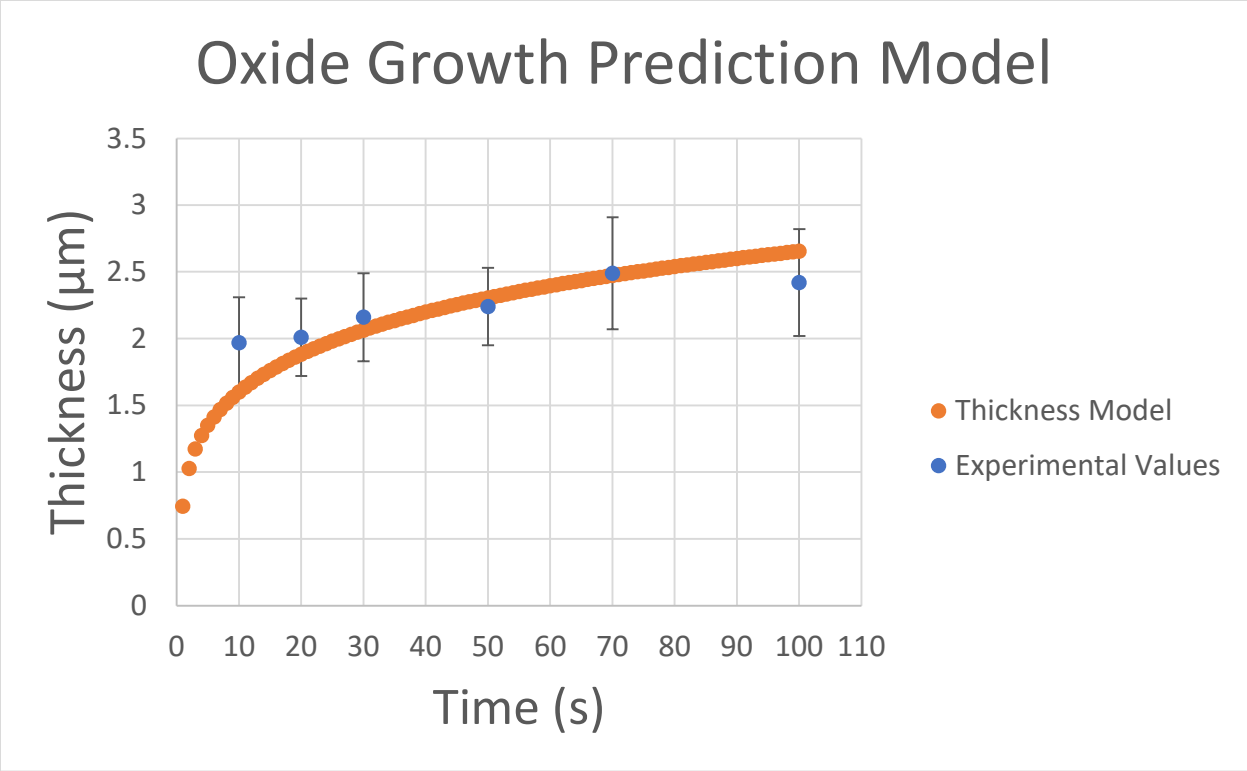

Figure 4.15: Oxide Growth Prediction Model compared to 450 V thickness data

4.5 Charge Density Analysis

Another important aspect of the coating process that was explored was the charge density that went through the uninsulated region of the sample. The charge density can be found by taking the integral, with respect to time, of the current density decay graphs. The charge density is the charge (current density x time) that passes through the surface per unit area in units of mC/cm^2. Figure 4.16 shows the relationship between charge density and time for all applied voltage levels. As voltage increases the overall charge density and rate at which charge density changes increases. The charge density curves flatten out quicker at lower voltage of 300 V, while 450 V still has some potential oxide growth at longer times.

The thickness measurements were also plotted next to the charge density data in figure 4.16 to determine possible correlation between charge density and coating thickness. The 450, 350 and 300 V thickness measurements align very well with the charge density variation. However, the 400 V shows a deviation with the expected coating thickness values being higher than the experimental. This might be due to the thickness and charge density being scaled differently on separate y-axes. The trend that the thickness measurements and charge density seem to be followed well for all voltages. The rate of increases between the charge density and thickness data can be seen to be similar for 450, 400, 350 and 300 V.

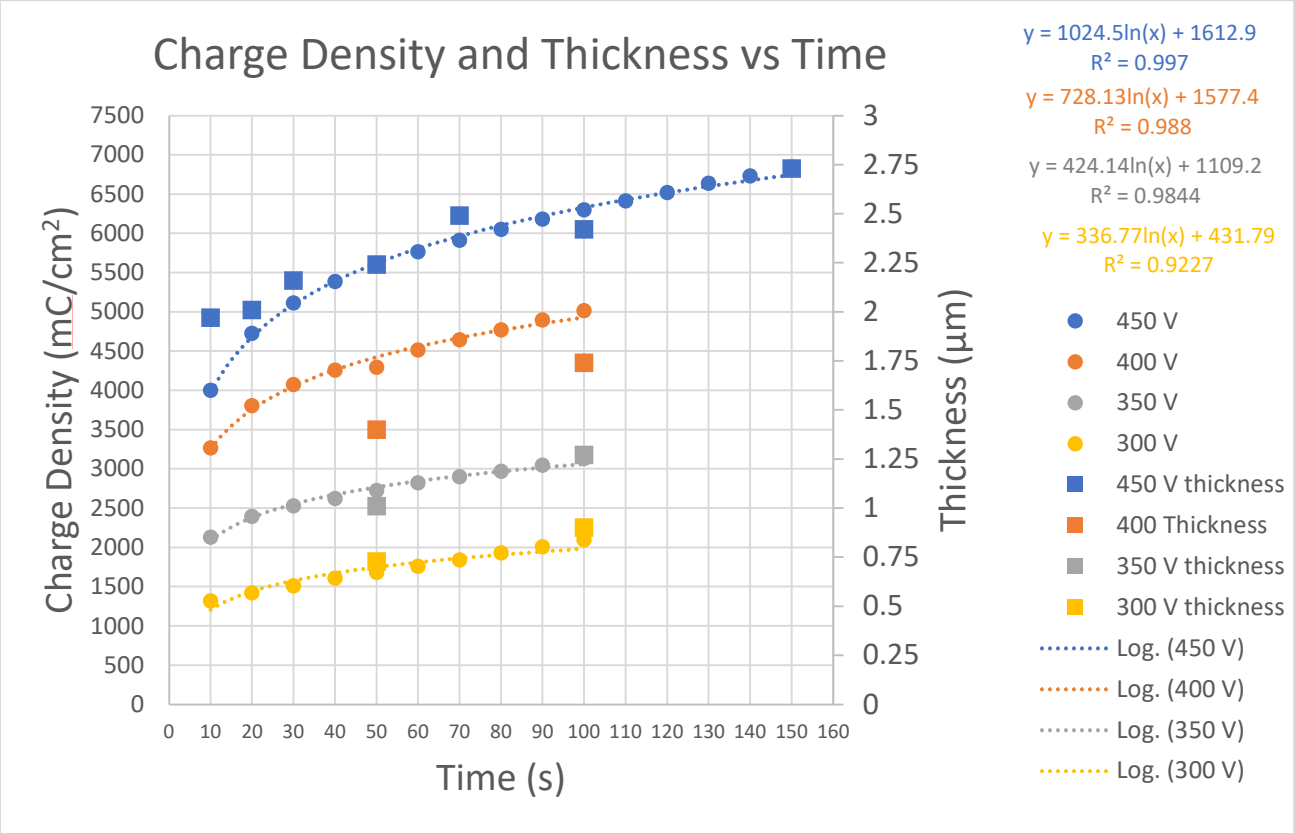

Figure 4.16: Charge Density vs Time and Thickness vs Time compared for all voltages

As noted earlier, the current during PEO is composed of ionic (contributing to coating thickness) and electronic (providing heating). A model of Ionic Charge Density versus time was also made by Kingsley in the SaNEL group. The model of Ionic Charge Density shows the expected Ionic Charge Density with respect to time, shown in orange in figure 4.17. The blue points in the same figure are the experimental Charge Density obtained from the 450 V 100 s experiment. These points obtained from that experiment are the overall total Charge Density. The coating thickness growth follows very well the trend of the ionic charge density predicted by the model. Subtracting the Ionic Charge Density model from the experimental data should give the Electronic Charge Density. Using this model, the Electronic Charge Density was obtained from the experimental data. This model can be further used to help make models at other Voltages, but further research and modeling would be required.

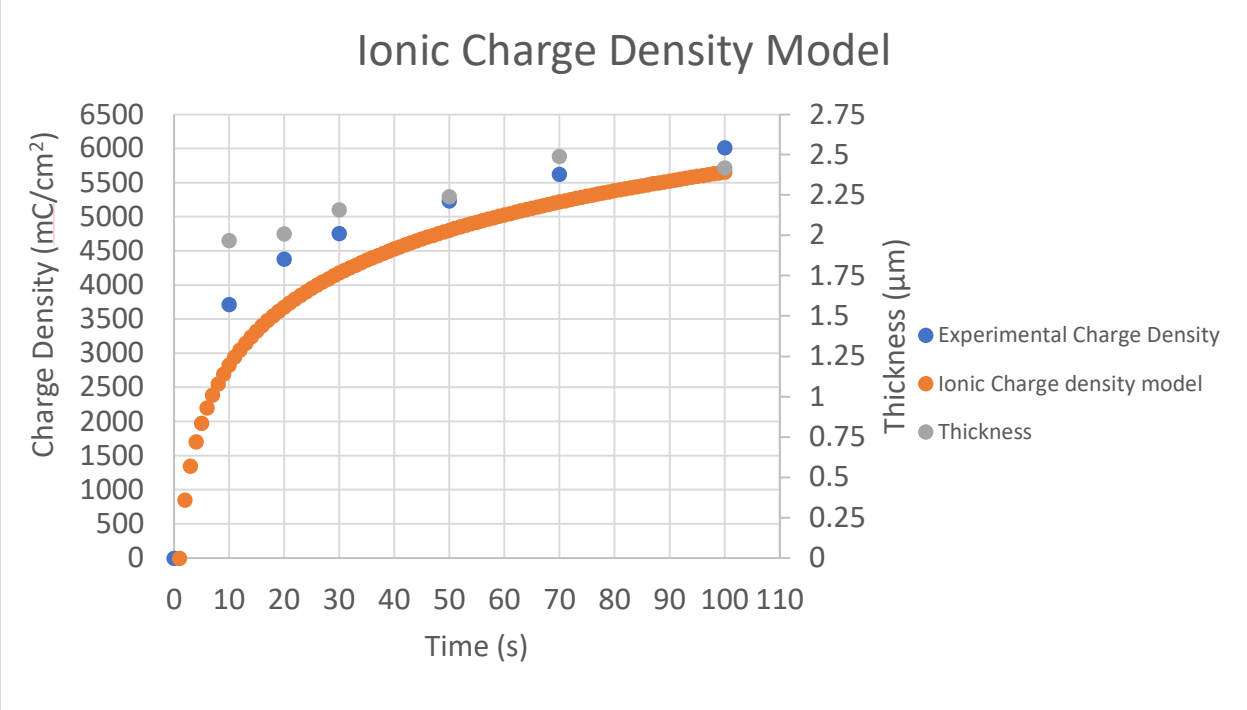

Figure 4.17: Experimental Charge Density compared with Ionic Charge Density Model. 450 V thickness measurements also included.

Finally, a plot of Charge Density vs Thickness was produced by using all the data obtained over all experiments (different voltage values and processing time). This plot is shown in figure 4.18. The results show a clear trend and correlation between charge density and coating thickness for the entire spectrum of different voltage levels applied and different processing time. As the voltage and time increases the charge density and thickness both increase as well. Based on the graph, the relationship between thickness and Charge Density appears to be linear. Using this relationship, the coating thickness can be predicted by measuring the charge density.

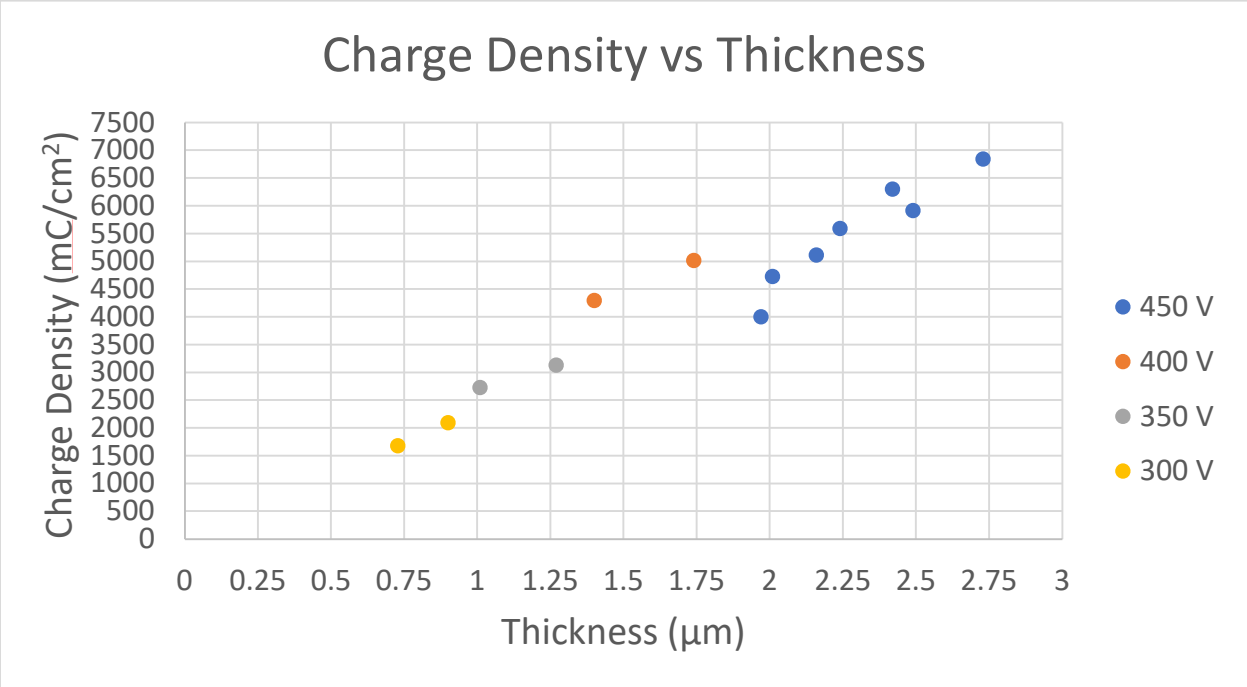

Figure 4.18: Experimental Charge Density vs Thickness for all 450, 400, 350 and 300 V.

CHAPTER 5

CONCLUSIONS

- Accurate oxide thickness measurements were made as a function of applied voltage and PEO processing time.
- Oxide coating exhibits a more significant increase in growth rate at higher voltage.
- Higher average current density prevails during processing at shorter times.
- Oxide layer is made up of several Ti oxides and amorphous phosphate phase.
- The thickness measurements, current density decay and charge density during PEO provided valuable data to assist the modeling effort.
- As the charge density applied increases the coating thickness increases.
- A good correlation between charge density and coating thickness was observed for all voltage levels applied and processing time. This relation can be used for predicting coating thickness directly from the PEO experimental parameters.

REFERENCES

[1] Jouanny, I., Labdi S., Aubert P., Buscema C., Maciejak O., Berger M. -H., Guipont V., and Jeandin M. “STRUCTURAL AND MECHANICAL PROPERTIES OF TITANIUM OXIDE THIN FILMS FOR BIOMEDICAL APPLICATION.” Thin Solid Films, vol. 518, no. 12, 2010, pp. 3212–3217., doi:10.1016/j.tsf.2009.09.046.

[2] Mortazavi, Golsa. “INVESTIGATION OF THE PLASMA ELECTROLYTIC OXIDATION MECHANISM OF TITANIUM.” The University of Texas at Arlington, 2017.

[3] Carmilla G. Dariva and Alexandre F. Galio, “CORROSION INHIBITORS – PRINCIPLES, MECHANISMS AND APPLICATIONS,” Developments in Corrosion Protection, Pgs. 365-380, 2014, doi: 10.5772/57255

[4] Boonrawd, Wisanu. “SURFACE MODIFICATION OF TITANIUM BY ELECTROLYTIC PLASMA PROCESSING AND IN-VITRO STUDIES.” The University of Texas at Arlington, 2021.

[5] Twaddle, Joshua. “PLASMA ELECTROLYTIC OXIDATION OF TITANIUM UNDER CONSTANT APPLIED VOLTAGE.” The University of Texas at Arlington, 2020.

[6] Kim, H., Koh Y., Li L., Lee S., and Kim H. “HYDROXYAPATITE COATING ON TITANIUM SUBSTRATE WITH TITANIA BUFFER LAYER PROCESSED BY SOL–GEL METHOD.” Biomaterials, vol. 25, no. 13, 2004, pp. 2533–2538., doi:10.1016/j.biomaterials.2003.09.041.

[7] Chen, Jim-Shone, Horng-Yih Juang, and Min-Hsiung Hon. “CALCIUM PHOSPHATE COATING ON TITANIUM SUBSTRATE BY A MODIFIED ELECTROCRYSTALLIZATION PROCESS.” Journal of Materials Science: Materials in Medicine, vol. 9, no. 5, 1998, pp. 297–300., doi:10.1023/a:1008825926440.

[8] Mortazavi G., Jiang J., and Meletis E. I. “INVESTIGATION OF THE PLASMA ELECTROLYTIC OXIDATION MECHANISM OF TITANIUM.” Applied Surface Science, vol. 488, 2019, pp. 370–382., doi:10.1016/j.apsusc.2019.05.250.

[9] Yerokhin et al. “PLASMA ELECTOLYSIS FOR SURFACE ENGINEERING.” Materials Science, Surface and Coatings Technology, December 1999. doi: 10.1016/s0257-8972(99)00441-7

[10] Smith, A., Kelton R., and Meletis E. I. “DEPOSITION OF NI COATINGS BY ELECTROLYTIC PLASMA PROCESSING.” Plasma Chemistry and Plasma Processing, vol. 35, no. 6, 2015, pp. 963–978., doi:10.1007/s11090-015-9642-9.

[11] Smith, Adam J. “SURFACE MODIFICATION OF IRON AND ALUMINUM BY ELECTROLYTIC PLASMA PROCESSING.” The University of Texas at Arlington, 2014.

[12] Ma X., Blawert C., Hoche D., Kainer K. U., and Zheludkevich M. L. “A MODEL DESCRIBING THE GROWTH OF A PEO COATING ON AM50 MG ALLOY UNDER CONSTANT VOLTAGE MODE.” Electrochimica Acta, vol. 251, 2017, pp. 461–474., doi:10.1016/j.electacta.2017.08.147.

[13] Murray, J. L., and H. A. Wriedt. “THE O−TI (OXYGEN-TITANIUM) SYSTEM.” Journal of Phase Equilibria, vol. 8, no. 2, 1987, pp. 148–165., doi:10.1007/bf02873201.

[14] Jung, Y.C., Shin, K.R., Ko, Y.G., Shin, D.H. “SURFACE CHARACTERISTICS AND BIOLOGICAL RESPONSE OF TITANIUM OXIDE LAYER FORMED VIA MICRO-ARC OXIDATION IN K3PO4 AND NA3PO4 ELECTROLYTES.” Journal of Alloys and Compounds, vol. 586, 2014, doi:10.1016/j.jallcom.2013.01.060.

[15] Shokouhfar, M., Dehghanian, C., Montazeri, M., Baradaran, A. “PREPARATION OF CERAMIC COATING ON TI SUBSTRATE BY PLASMA ELECTROLYTIC OXIDATION IN DIFFERENT ELECTROLYTES AND EVALUATION OF ITS CORROSION RESISTANCE: PART II.” Applied Surface Science, vol. 257, no. 7, 2011, pp. 2617–2624., doi:10.1016/j.apsusc.2010.10.032.

BIOGRAPHICAL INFORMATION

In 2019, Hunter graduated from The University of Arizona with a B.S. degree in Chemistry. While at The University of Arizona he worked in Dr. Lichtenberger's research lab doing research on synthesis of Organometallic small molecule catalysts. After graduating from The University of Arizona he started pursuing a M.S. degree in Materials Science and Engineering from the University of Texas at Arlington.